CLIC-dependent internalization of caveolin-1 to lysosomal vacuoles in response to osmotic regulation

Timothy H. Wong[1], Aditya Nagrath[1], Matheus F. Lima[1], Y. Lydia Li[1], Bharat Joshi[1], Ivan Robert Nabi[1,2*]

[1]Department of Cellular & Physiological Sciences, Life Sciences Institute, University of British Columbia, Vancouver, BC, Canada V6T 1Z3
[2]School of Biomedical Engineering, University of British Columbia, Vancouver, BC, Canada V6T 1Z3

[*]To whom correspondence should be sent: irnabi@mail.ubc.ca

Keywords: caveolae, caveolin-1, CLIC endocytosis, lysosome, osmotic shock

Abstract

Originally thought to be a major endocytic portal, a major function of caveolae is now considered to be a membrane buffer, in which flattening of caveolae protects the plasma membrane from rupture under mechanical stress, such as hypotonic shock. However, the fate of Cav1 in response to hypotonic shock is not known. Here, we show that extended hypotonic shock results in the robust, ubiquitin-independent, CLIC-dependent endocytosis of Cav1 to form large, intracellular, Cav1-positive lysosomal vacuoles that are positive for the lysosomal marker LAMP1 and negative for MVB markers and the acidic lysosome indicator Lysosensor. Cav1 recycles from these lysosomal vacuoles to the plasma membrane upon return to isotonic conditions. Cav1 internalizes not in response to initial cell expansion upon hypotonic shock but rather subsequent reduction of cell volume. Upon hypertonic shock, Cav1 internalization occurs selectively in PC3 cells, that lack caveolae and the caveolar adaptor protein cavin-1, and is inhibited upon cavin-1 reintroduction. CLIC endocytosis of non-caveolar Cav1 to neutral pH lysosomes in response to osmotic regulation defines a novel recycling pathway for Cav1 to enable caveolae membrane buffering function.

Introduction

Caveolae were first identified by EM as smooth invaginations of the plasma membrane in the 1950's and thought to be an endocytic portal, particularly in endothelial cells [1-3]. However, the contribution of caveolae endocytosis to total endocytosis is relatively low and specific cargo for caveolae endocytosis have been difficult to identify, challenging the role of caveolae as a major endocytic portal [3, 4]. Caveolae were previously suggested to mediate the endocytosis of SV40 virus to a distinct Cav1-positive organelle, the caveosome, prior to viral delivery to the ER [5]. Caveosomes were considered a distinct endocytic organelle as they were pH neutral and not labeled for early endosomal or lysosomal markers [5]. However, the same authors subsequently identified the ubiquitin-dependent endocytosis of Cav1, showing that Cav1 ubiquitination promoted its endocytosis via multivesicular bodies to lysosomes for degradation [6]. The caveosome was therefore considered to be an artifact of Cav1-GFP overexpression [6, 7].

Indeed, a major function of caveolae is now considered to be not endocytosis but rather a membrane buffer, in which flattening of caveolae protects the plasma membrane from rupture under mechanical stress, such as hypotonic shock or cell stretching [8-11]. Caveolae flattening in response to hypotonic shock results in dissociation of the Cavin-1 adaptor, required for caveolae formation [8]. Cav1 forms non-caveolar membrane structures or Cav1 scaffolds [12], including the disk-like 11-mer 8S complex recently characterized by cryoEM as well as larger 8S homo-oligomers [13-16]. Dissociation of Cavin-1 from caveolae upon hypotonic shock is associated with increased dynamics of the released non-caveolar Cav1 scaffold domains as well as scaffold interaction with and inhibition of JAK-STAT signaling [17]. However, the fate of disassembled

Cav1 in response to hypotonic shock and how Cav1 can reform caveolae to protect the membrane against multiple cycles of stretch is not known.

Here, we show that extended hypotonic shock results in the CLIC-dependent endocytosis of Cav1 to form large, intracellular, pH neutral, Cav1-positive lysosomal vacuoles that resemble the previously described caveosome. Cav1 internalization occurs independently of cavin-1, and therefore of caveolae, and of Cav1 ubiquitination; our data suggest that Cav1-positive lysosomal vacuoles are not an endosomal sorting station but rather a recycling lysosomal reservoir. Indeed, Cav1 endocytosis occurs not in response to cell expansion due to hypotonic shock but rather upon subsequent reduction of cell volume, consistent with previous reports of upregulated CLIC endocytosis in response to reduced cell volume [18]. Cav1 scaffold endocytosis to Cav1-positive, pH neutral, lysosomal vacuoles defines a robust non-caveolar Cav1 recycling pathway to enable multiple rounds of caveolae buffering in response to osmotic regulation of cell volume.

Results

Caveolae have been demonstrated to flatten in epithelial HeLa cells, mouse lung endothelial cells (MLECs), mouse embryonic fibroblasts (MEF) and mouse brain endothelial derived bEnd5 cells treated with acute (5-15 minutes) hypotonic shock protecting the membrane from rupture in response to mechanical stress [8, 9, 19]. Here, we used fixed cell TIRF to analyze the cell surface response of endogenous Cav1 to hypotonic shock over 60 minutes in MDA-MB-231 breast cancer cells. Cav1 surface expression progressively decreased over 60 minutes compared to cells imaged under isotonic conditions and recovered after 60 minutes upon addition of isotonic

medium after 60 minutes of hypotonic shock (Figure 1A). Using fixed cell STED imaging of Cav1, we observed Cav1 puncta at the cell membrane under isotonic conditions; in cells treated with hypotonic shock, Cav1 localized to large spherical vacuoles that appeared at 15 minutes hypotonic shock and increased in abundance to 60 minutes (Figure 1B). These vacuoles were not visible by TIRF microscopy suggesting that they are intracellular and do not correspond to the recently described doline [20]. In the absence of cavin-1, Cav1 has been demonstrated to be endocytosed with CD44 via the CLIC/GEEC pathway [21]. We therefore tested whether the hypotonic induced Cav1-positive vacuoles were positive for CD44 and the CLIC/GEEC cargo, β1 integrin, whose expression, signaling and endocytosis are regulated by Cav1 [22-26]. While both CD44 and β1-integrin show a surface distribution under isotonic conditions, following 60 minutes of hypotonic shock both CD44 and β1-integrin localize to Cav1 spherical vacuoles (Figure 1C). The average diameter of spherical vacuoles positive for Cav1 CD44 and β1-integrin was 0.97 µm and ranged from ~0.3-3µm (Figure 1C).

To confirm that these spherical vacuoles are endocytic in nature, we performed an acid wash internalization assay using anti-CD44 and anti-β1 integrin antibodies (Figure 2A). Antibodies were added to hypotonic or isotonic media and, at the indicated times, cells were acid-stripped to remove the surface antibody labelling and then fixed. As a control, antibodies were added in isotonic media at 4°C to prevent endocytosis for 60 minutes. Fluorescent labeling showed surface labelling of CD44 and β1 integrin without acid wash, that was completely removed by acid stripping at 4°C, demonstrating that the acid wash is removing surface labeling of CD44 and β1 integrin. Significantly increased internalization was detected for β1 integrin and CD44 antibodies at 15-, 30- and 60 minutes post hypotonic shock relative to internalization under

isotonic conditions for 60 minutes (Fig. 2A). Cav1 endocytic vacuoles are observed associated with internalized CD44 and β1 integrin (Fig. 2A, insets). Extent of overlap of a Cav1 mask with internalized CD44 and β1 integrin labelling increased over time in hypotonic medium and was significantly increased at 15-, 30- and 60 minutes post hypotonic shock relative to isotonic medium at 37°C (Fig. 2A). Dominant negative CDC42 has been shown to be a specific inhibitor of CLIC/GEEC endocytosis [27, 28]. Expression of wild-type CDC42 did not impact Cav1 endocytosis and CDC42-GFP associated with Cav1 endocytic vacuoles. In contrast, dominant negative CDC42 mutant prevented the formation of Cav1 vacuoles (Figure 2B). In response to long durations of hypotonic shock, Cav1 is therefore endocytosed via the CLIC/GEEC endocytic pathway.

Ubiquitin-dependent trafficking of Cav1 to lysosomes via multivesicular bodies (MVBs) has been reported [6]. We therefore expressed LAMP1-GFP and found that upon hypotonic shock more than 50% of Cav1 endocytic vacuoles colocalized with LAMP-GFP (Figure 3A). To determine whether ubiquitination is required for Cav1 endocytic vacuole formation we expressed, in Cav1 knockout MDA-MB-231 cells [29], HA-tagged wild-type Cav1-HA or the Cav1-K*R-HA mutant in which all lysine residues are mutated to arginine, that was previously shown to prevent Cav1 ubiquitination and internalization to lysosomes [6], In response to hypotonic shock, the Cav1-K*R-HA ubiquitin mutant localized to Cav1-positive endocytic vacuoles to the same extent as wild-type Cav1-HA, indicating that Cav1 ubiquitination is not required for osmotic regulated Cav1 endocytosis (Figure 3B). Consistently, Cav1/CD44 positive vacuoles are labelled for endogenous LAMP1 and negative for the MVB markers CD63 and LBPA, further supporting that Cav1/CD44 vacuoles are not MVBs (Supplemental Figure S1).

To determine whether Cav1-positive lysosomal vacuoles are acidic, we performed live cell experiments of cells expressing Halo-tagged Cav1, labeled with Halo ligand LIVE RED, and LAMP1-mScarlet and incubated the cells with the acid-dependent lysosomal reporter LysoSensor green. Under isotonic conditions, LAMP1-mScarlet lysosomes are strongly labeled for both LAMP1 and LysoSensor and poorly labeled for Cav1-Halo. However, under hypotonic shock, LAMP1-mScarlet lysosomes are strongly labeled for Cav1-Halo and poorly labeled for LysoSensor (Figure 3C). Similarly, upon treatment with bafilomycin A1 (BafA), a V-ATPase inhibitor that neutralizes endolysosomal pH, cells under isotonic conditions contain LAMP-1-positive lysosomes poorly labelled for LysoSensor. Further, BafA inhibition of lysosome acidification did not prevent the formation of Cav1 lysosomal vacuoles. Taken together, these results indicate that in response to hypotonic shock Cav1 is trafficked into pH-neutral lysosomal vacuoles independently of Cav1 ubiquitination.

Assessment of cell volume changes using quantitative phase imaging microscopy showed that cell volume spiked within five minutes after hypotonic shock and then decreased below the initial isotonic cell volume, plateauing at a reduced cell volume after about 15 minutes hypotonic shock (Figure 4A). These results suggest that Cav1 endocytosis does not occur during initial cell swelling upon hypotonic shock but rather during the subsequent decrease in cell volume. To investigate whether Cav1 endocytic vacuoles form in response to decreasing cell volume, we applied both hypertonic and hypotonic shock to MDA-MB-231 cells as well as PC3 prostate cancer cells, that lack cavin-1 and do not form caveolae [30]. MDA-MB-231 cells accumulated

spherical Cav1-positive lysosomal vacuoles over 15-60 minutes post-hypotonic shock as described previously, but did not form Cav1 lysosomal vacuoles upon hypertonic shock (Figure 4B). In PC3 cells, Cav1-positive lysosomes formed at 5 and 15 minutes post-hypotonic shock and, in contrast to MDA-MB-231 cells, Cav1-positive lysosomal vacuoles accumulated over time in PC3 cells under hypertonic shock. To test whether cavin-1 expression is limiting Cav1 endocytosis in response to hypertonic shock, we expressed cavin-1-GFP in PC3 cells. Under hypertonic shock, cells expressing cavin-1-GFP no longer formed Cav1 lysosomal vacuoles, whereas under hypotonic shock, Cav1 still trafficked to lysosomal vacuoles (Figure 4C). Dissociation of cavin-1 from Cav1 upon caveolae flattening in response to hypotonic shock [8], is therefore necessary for Cav1 endocytosis in response to subsequent cell shrinking. Upon hypoosmotic shock, caveolae flattening releases non-caveolar scaffolds that are internalized following membrane relaxation via CLIC endocytosis to neutral pH lysosomes, from which Cav1 can return to the plasma membrane to reform caveolae for subsequent rounds of membrane stretch.

Discussion

We show here that in response to extended hypotonic shock, Cav1 is robustly and reversibly internalized via CLIC endocytosis to neutral pH lysosomal vacuoles in a caveolae-independent manner. Loss of cavin-1 and caveolae disassembly increase Cav1 lateral mobility and rate of degradation [6, 30, 31]. However, we observe that Cav1 lysosomal vacuoles are negative for the acidic pH indicator Lysosensor and upon return to isotonic conditions, Cav1 efficiently recycles

to the plasma membrane. Furthermore, a lysine-free Cav1 mutant, unable to be ubiquitinated, is efficiently internalized in response to hypotonicity; osmotically regulated Cav1 endocytosis is therefore distinct from ubiquitin-dependent endocytosis of Cav1 to lysosomes for degradation [6]. Tracking cell volume in response to hypotonic shock demonstrates that Cav1 endocytosis and endocytic vacuole formation are occurring as cells acclimatize to hypotonic shock and decrease cell volume. Similarly, other studies measuring cell volume in response to hypotonic shock show that ion channel compensation decreases cell volume in response to the initial volume spike caused by hypotonic shock [32, 33]. Indeed, cell growth on soft substrates, associated with reduced cell spreading and volume, has been reported to be associated with Cav1 endocytosis [34, 35].

Our data define a Cav1 recycling pathway in response to hypoosmotic shock: 1. caveolae flatten to buffer membrane stretch and release cavin-1 to form Cav1 scaffolds; 2. scaffolds then internalize via CLIC endocytosis to pH neutral lysosomal vacuoles; and 3. Cav1 recycles to the plasma membrane to enable reformation of caveolae. Cav1 has been shown to be internalized via the CLIC pathway in the absence of cavin-1, and indeed cavin-1 shown to inhibit its endocytosis [21]. Consistently, in PC3 cells lacking cavin-1, Cav1 endocytosis occurs in response to hyperosmotic shock and is prevented by reintroduction of cavin-1. The CLIC pathway has a high capacity for endocytosis, responds to and regulates membrane tension and is a major contributor to fluid-phase uptake in response to mechanical stress [18, 36]. Interestingly, vinculin regulates fluid uptake via CLIC/GEEC during recovery following osmotic shock [18], Cav1 modulates vinculin focal adhesion tension [37] and Cav1 inhibits CLIC endocytosis [21]. Cav1 therefore sits at the intersection of two mechanosensitive mechanisms, caveolae flattening and

CLIC/GEEC endocytosis, both implicated in the cellular response to mechanical and osmotic stress. CLIC-dependent, non-caveolar endocytosis of Cav1 to neutral pH lysosomal vacuoles in response to osmotic changes represent a robust recycling pathway for Cav1 in response to altered membrane tension that may enable repeated caveolae membrane buffering.

While the Cav1-positive neutral pH lysosomal vacuoles reported here resemble the previously described "caveosome" [5], they are not an endocytic sorting compartment but rather an intracellular recycling compartment for cellular management of cell volume changes in response to changes in osmotic pressure, similar to reservoirs or vacuole-like dilations [18, 38]. Indeed, LAMP-1-positive and Lysotracker-negative vacuoles were recently reported to form 30 minutes following hypotonic shock, accumulating over 6 hours [39]. Upon hypotonic shock, lysosomes can act as intracellular water storage vacuoles regulated by the volume-regulated anion channel LLRC8A, contributing to cell volume decreases and cell survival [31, 40]. Rapid caveolae endocytosis has been reported to repair plasma membrane wounds in association with Ca^{++}-dependent exocytosis of lysosomes; loss of Cav1 impairs wound repair and is associated with enhanced Endophilin A2 endocytosis [41-43]. How this membrane repair pathway of Cav1 endocytosis relates to that reported here in response to osmotic shock is not clear, however our data argues that Cav1 endocytosis in response to osmotic shock is scaffold, and not caveolae, mediated. Of interest, downregulation of both Cav1 and cavin-1 were shown to increase the expression of matrix proteases and glioblastoma invasion in response to increased hydrostatic pressure [44]. Whether Cav1 impacts the dynamics or function of this organelle or is simply a bystander cargo internalized upon induction of CLIC endocytosis upon membrane relaxation for recycling to reform membrane caveolae remains to be determined.

Materials and Methods

Antibody and plasmids

Primary antibodies: rabbit anti-Cav1 mAb (3267) was purchased from Cell Signaling Technology, rat anti-CD44 mAb (22530) from Novus, and mouse anti-β1 integrin mAb (sc-53711) from Santa Cruz. Secondary antibodies: goat anti-rabbit Alexa488 (A32731), goat anti-mouse Alexa488 (A32723), goat anti-rabbit Alexa532 (A-11009), goat anti-mouse Alexa532 (A11002) and goat anti-rat Alexa568 (A11077) were purchased from ThermoFisher. LAMP1-mGFP (#34831), LAMP1-mScarlet (#98827), and Cavin1-GFP (#68401) plasmids were obtained from Addgene. CDC42-myc wild-type and dominant negative (N17) plasmids were a generous gift from Nathalie Lamarche (McGill University). In order to generate dually tagged Halo and Myc human Cav-1, Cav1-myc and Halo Tag containing pST018 (a gift from Sheila Teves, UBC) were used as template DNAs and PCR (Platinum Taq, Invitrogen) amplified following overlapping extension method using a set of forward and reverse primers (5'GGA AGC TTA GCA TGT CTG GGG GCA AAT AC3' 5'CGG CCG GTC GCC ACC ATG GCA GAA ATC GGT3'; 5'ACC GAT TTC TGC CAT GGT GGC GAC CGG CCG3', 5'GAA TTC TTA CGT ACG CTT GTC GTC ATC GTC TTT GTA GTC3'). The PCR products were TA cloned and plasmids sequence verified to check fusion of Halo tag with Cav1-Myc. The correct sequence containing Cav1-Myc-Halo fragment was released from the TA-clone using EcoR1 and re-cloned into pcDNA3 at the EcoR1 site. Positive clones were sequence verified for the correct orientation and used for the transfection and subsequent experiments.

Cell culture, transfection, osmotic shock and drug treatments

Generation and characterization of the cloned MDA-MB-231 and PC3 cell lines and the Cav1 knockout cell lines used in this study were as described previously [45, 46]. All cell lines were tested regularly for mycoplasma infection by PCR (ABM, Richmond, BC, Canada). Cell lines were grown in Gibco™ RPMI-1640 medium (CAT#21870076) that was supplemented using 10% fetal bovine serum (FBS) and 2□mM□L-glutamine (ThermoFisher). MDA-MB-231 cells were passaged using 0.05% Trypsin-EDTA (ThermoFisher) and 0.25% for PC3 cell lines and used for a maximum of ten passages. For plasmid transfections, cells were seeded for 24 h and then transfected overnight using Lipofectamine 2000 (Life Technologies, Thermo Fisher Scientific) as described by the manufacturer's protocol. For live cell confocal imaging, cells were seeded for 24 h on an 8-well #1.5H glass bottom slide (Ibidi). Transfection was performed overnight as described above.

Cells grown on #1.5H 18mm square coverslips (Paul Marienfeld, Lauda-Königshofen, Germany). were treated with osmotic shock after being seeded for 48 h. For hypoosmotic shock (30 mOsm), complete media (300 mOsm) was diluted 1:10 with MQ water and treated for the time duration as described. For hyperosmotic shock (500 mOsm), 2M NaCl solution was diluted 1:10 with complete media. Where indicated, before imaging, cells were pre-treated with 100nM BafA (Sigma Aldrich C1988) for a total of 2 h and kept in media containing BafA for subsequent incubations and for imaging. Cells were then incubated for 30 minutes with 1uM LysoSensor

green (ThermoFisher L7535) and LIVE RED Halotag ligand (Abberior LVRED-0147-30NMOL) as indicated before being washed 3x with HEPES buffered DMEM without phenol red (ThermoFisher 21063-029). Multiple cells were imaged over a period of 30 minutes in isotonic DMEM or after 30 minutes of osmotic shock.

Acid-wash internalization assay

Internalization assays were adapted from Chaudhary *et al.* [21]. Cells were grown on coverslips in 6 well plates before being transferred to a 150mm dish lined with parafilm. Cells were treated with a 250 µl solution of isotonic or hypotonic media containing 10 µg/ml anti-CD44 and anti-β1 integrin antibody and incubated for the indicated times. To remove uninternalized and surface bound antibodies, acid stripping was performed using 2x30 second washes in 0.5 M glycine at pH 2.2. Cells were then fixed with 4% paraformaldehyde for 15 minutes and labeled with anti-Cav1 primary and secondary antibodies.

Fluorescence labeling and imaging

Cell fluorescence labeling and STED imaging was performed as previously described [47]. Briefly, cells were permeabilized using 0.2% Triton X-100 (Sigma) and blocking was performed for 1 h with 10% goat serum (ThermoFisher) and 1% bovine serum albumin (Sigma). Coverslips were incubated with primary antibodies (diluted in antibody buffer containing 10% goat serum, 1% BSA, and 0.05% Triton-X100 in saline-sodium citrate buffer) overnight at 4°C and then washed with antibody wash buffer containing saline-sodium citrate buffer and 0.05% Triton-X100. Fluorescent secondary antibodies were incubated for 1h at room temperature and washed with antibody wash buffer before being mounted with ProLong™ diamond antifade mountant

(ThermoFisher). STED and live cell confocal imaging was carried out using a Leica SP8 microscope with a 100×/1.4 Oil HC PL APO CS2 STED White objective. STED and confocal images were deconvolved using Huygens Professional software (Scientific Volume Imaging). TIRF imaging was performed using a Leica SR GSD 3D system using a 160□×□objective lens (HC PL APO 160□×□/1.43, oil immersion) with TIRF illumination.

Volume Phase Imaging

Cells were seeded for 48h on µ-Slide VI 0.5 Glass Bottom (1.5H) from Ibidi. A gravity mount ant perfusion was set up by adapting a Ibidi perfusion set (white). Imaging was performed with a HoloMonitor (PHI) quantitative phase imaging microscope placed inside a cell culture incubator culture incubator at 37°C and 5% CO2. Cells were imaged for 5 minutes under isotonic media and was exchanged with the prepared hypoosmotic media. 8-10 ROIs were selected and images were acquired every 30 seconds. Cells were segmented, tracked, and quantified at each timepoint using the HoloMonitor software package. A single cell tracking module was applied and 7-10 cells were selected from each ROI for quantification. Cells were selected based on the software being able to sufficiently isolate the single cell by segmentation and track the same cell for the entire duration of the experiment.

Quantification and statistical analysis

Quantification of TIRF Cav1 fluorescence was performed with ImageJ/FIJI. Quantification of Cav1-positive endocytic vacuoles was done by manual scoring. Quantification of internalization assays and area overlap was performed using the ImageJ plugin JACoP [48]. Graphs and statistical analyses were performed using GraphPad Prism (GraphPad Software, San Diego, CA). Statistical tests used are indicated in the figure legends.

Acknowledgements

This study was supported by a grant from the Canadian Institutes of Health Research (IRN: PJT-175112).

Figure Legends

Figure 1. Hypotonic shock induces reversible internalization of Cav1

A) MDA-MB-231 cells were incubated in isotonic media, in hypotonic media for 5, 15, 30 and 60 minutes or under Recovery conditions in which hypotonic media was replaced after 60 minutes with isotonic media for 5, 15, 30 or 60 minutes. Cells were labeled for Cav1, fixed and imaged by TIRF widefield imaging. Average Cav1 intensity per cell was quantified and normalized to isotonic control. Representative images of select conditions are shown. (n=3 independent experiments with >30 cells for each condition; ANOVA with Dunnett's post-test comparing to isotonic control; **$p < 0.01$; ***$p < 0.001$; Scale bar: 2µm). B) STED imaging of anti-Cav1 labeling MDA-MB-231 cells incubated in isotonic media or in hypotonic media for 15 or 60 minutes. Cav1 endocytic vacuoles were counted per cell. (n>28 from three independent experiments for isotonic and hypotonic 15 minutes, four independent experiments for other conditions; (ANOVA with Dunnett post-test comparing to isotonic control; *$p < 0.05$; ****$p < 0.0001$; Scale bar: 4µm; Inset scale bar: 1µm). C) MDA-MB-231 cells incubated with isotonic or hypotonic media for 60 minutes were fixed and labeled for Cav1, CD44 and β1-integrin (Scale bar: 4µm). The diameter of individual Cav1, CD44, and β1-integrin positive endosomes was measured from three independent experiments.

Figure 2. Cav1 is endocytosed via the CLIC pathway in response to hypotonic shock

A) MDA-MB-231 cells were incubated with anti-CD44 and anti-β1 integrin antibodies in isotonic media for 60 minutes at 4°C or 37°C or in hypotonic media for 5, 15, 30 or 60 minutes at 37°C. As indicated, an acid wash treatment was performed at 4°C to remove surface antibodies and cells were fixed and labeled with secondary antibodies to anti-CD44 and anti-β1 integrin as well as for endogenous Cav1. (n= >30 cells per condition from three independent experiments; ANOVA with Dunnett post-test comparing each condition to isotonic 4°C control; *$p < 0.05$; ***$p < 0.001$; ****$p < 0.0001$; Scale bars: 2 µm). B) MDA-MB-231 cells were transfected with wild-type CDC42-GFP or dominant negative (Dom Neg) CDC42-GFP, incubated with isotonic or hypotonic media for 60 minutes and then fixed and labeled for Cav1 and CD44. CDC42-GFP was also imaged and the number of Cav1 endocytic vacuoles counted per cell (n>30 cells from three independent experiments; ANOVA with Dunnett's post-test comparing to isotonic control; ****$p < 0.0001$; Scale bar: 2µm).

Figure 3. Ubiquitin-independent endocytosis of Cav1 to pH neutral lysosomes

A) MDA-MB-231 cells were transfected with LAMP-GFP, incubated with isotonic or hypotonic media for 60 minutes and then fixed and labeled for Cav1. LAMP-GFP was also imaged and the number of Cav1 endocytic vacuoles counted per cell (n>30 from cells three independent experiments with >30 cells for each condition; ANOVA with Dunnett's post-test comparing to isotonic control; ****$p < 0.0001$; Scale bar: 2 µm). B) Cav1 CRISPR knockout MDA-MB-231 cells were transfected with Cav1-WT-HA or Cav1-K*R-HA lysine mutant, incubated with isotonic or hypotonic media for 15 or 60 minutes and then fixed and labeled for Cav1 and CD44.

(n>29 cells from three independent experiments; ANOVA with Tukey post-test comparing WT to K*R at the same isotonic or hypotonic conditions and the respective hypotonic condition to isotonic control; Scale bar: 2µm). C) MDA-MB-231 cells were transfected with LAMP1-mScarlet and Cav1-Halo, where indicated pre-treated with 100nM BafA for 2 hours, labeled with Halo-LIVE RED for 30 minutes and then incubated for 30 minutes with 1uM LysoSensor green and LIVE RED Halotag ligand. Cells were then placed in isotonic or hypotonic imaging media and multiple cells imaged over a period of 30 minutes in isotonic DMEM or after 30 minutes of hypotonic shock. LysoSensor and Cav1 intensity within LAMP1-positive lysosomes were quantified. (n>38 cells from three independent experiments; ANOVA with Tukey's post-test; *p < 0.05; ****p < 0.0001; Scale bar: 2 µm).

Figure 4. Cavin1-independent Cav1 endocytosis is associated with reduced cell volume

A) Cell volume of MDA-MB-231 and PC3 cells switched from isotonic to hypotonic media was measured by live phase imaging. Black line indicates addition of hypotonic media (n=3 independent experiments; each experiment includes 2-3 technical replicates and each technical replicate consists of 9 ROIs). B) MDA-MB-231 and PC3 cells were incubated in isotonic media, or hypotonic or hypertonic media for 5, 15, 30 and 60 minutes. Cells were labeled for Cav1 and CD44 and Cav1 endocytic vacuoles counted per cell. Representative images for select time points are shown. (n>28 cells from three independent experiments; ANOVA with Dunnett's post-test comparing each condition to isotonic control; *p < 0.05; **p < 0.01; ****p < 0.0001; Scale bar: 2 µm). C) PC3 cells and PC3 cells stably transfected Cavin-1-GFP were incubated in isotonic, hypotonic and hypertonic shock media for 60 minutes and then fixed and labeled for Cav1. Cavin-1-GFP was imaged in the GFP channel and Cav1 endocytic vacuoles counted per

cell. (n>28 cells from three independent experiments; ANOVA with Tukey's post-test and comparing PC3 to PC3+Cavin-1 and each condition with the respective isotonic control; **p < 0.01; ***p < 0.001; ****p < 0.0001; Scale bar: 2 µm).

Supplemental Figure S1. Hypotonic shock induced Cav1/CD44 vacuoles are positive for endogenous LAMP1 and negative for MVB markers.

STED imaging of endogenous Cav1 in red, CD44 in blue, and either LAMP1, CD63 or LBPA in green, as indicated, in MDA-MB-231 cells incubated in either isotonic media or in hypotonic media for 60 minutes. Insets show triple labelled lysosomal vacuoles (Scale bar: 5µm; Inset scale bar: 2µm).

1. Palade, G.E. (1953). Fine structure of blood capillaries. Journal of Applied Physiology *24*, 1424.
2. Frank, P.G., Pavlides, S., and Lisanti, M.P. (2009). Caveolae and transcytosis in endothelial cells: role in atherosclerosis. Cell and Tissue Research *335*, 41-47.
3. Parton, R.G., del Pozo, M.A., Vassilopoulos, S., Nabi, I.R., Le Lay, S., Lundmark, R., Kenworthy, A.K., Camus, A., Blouin, C.M., Sessa, W.C., et al. (2020). Caveolae: The FAQs. Traffic *21*, 181-185.
4. Shvets, E., Bitsikas, V., Howard, G., Hansen, C.G., and Nichols, B.J. (2015). Dynamic caveolae exclude bulk membrane proteins and are required for sorting of excess glycosphingolipids. Nature Communications *6*, 6867.
5. Pelkmans, L., Kartenbeck, J., and Helenius, A. (2001). Caveolar endocytosis of simian virus 40 reveals a new two-step vesicular-transport pathway to the ER. Nat Cell Biol *3*, 473-483.
6. Hayer, A., Stoeber, M., Bissig, C., and Helenius, A. (2010). Biogenesis of caveolae: stepwise assembly of large caveolin and cavin complexes. Traffic *11*, 361-382.
7. Parton, R.G., and Howes, M.T. (2010). Revisiting caveolin trafficking: the end of the caveosome. J Cell Biol *191*, 439-441.
8. Sinha, B., Köster, D., Ruez, R., Gonnord, P., Bastiani, M., Abankwa, D., Stan, R.V., Butler-Browne, G., Vedie, B., Johannes, L., et al. (2011). Cells respond to mechanical stress by rapid disassembly of caveolae. Cell *144*, 402-413.
9. Cheng, J.P.X., Mendoza-Topaz, C., Howard, G., Chadwick, J., Shvets, E., Cowburn, A.S., Dunmore, B.J., Crosby, A., Morrell, N.W., and Nichols, B.J. (2015). Caveolae protect endothelial cells from membrane rupture during increased cardiac output. Journal of Cell Biology *211*, 53-61.
10. Parton, R.G. (2018). Caveolae: Structure, Function, and Relationship to Disease. Annual Review of Cell and Developmental Biology *34*, 111-136.
11. Singh, V., and Lamaze, C. (2020). Membrane tension buffering by caveolae: a role in cancer? Cancer Metastasis Rev *39*, 505-517.
12. Lajoie, P., Goetz, J.G., Dennis, J.W., and Nabi, I.R. (2009). Lattices, rafts, and scaffolds: domain regulation of receptor signaling at the plasma membrane. J Cell Biol *185*, 381-385.
13. Khater, I.M., Liu, Q., Chou, K.C., Hamarneh, G., and Nabi, I.R. (2019). Super-resolution modularity analysis shows polyhedral caveolin-1 oligomers combine to form scaffolds and caveolae. Sci Rep *9*, 9888.
14. Khater, I.M., Meng, F., Wong, T.H., Nabi, I.R., and Hamarneh, G. (2018). Super Resolution Network Analysis Defines the Molecular Architecture of Caveolae and Caveolin-1 Scaffolds. Scientific Reports *8*, 9009.
15. Han, B., Porta, J.C., Hanks, J.L., Peskova, Y., Binshtein, E., Dryden, K., Claxton, D.P., McHaourab, H.S., Karakas, E., Ohi, M.D., et al. (2020). Structure and assembly of CAV1 8S complexes revealed by single particle electron microscopy. Sci Adv *6*, eabc6185.
16. Porta, J.C., Han, B., Gulsevin, A., Chung, J.M., Peskova, Y., Connolly, S., McHaourab, H.S., Meiler, J., Karakas, E., Kenworthy, A.K., et al. (2022). Molecular architecture of the human caveolin-1 complex. Sci Adv *8*, eabn7232.
17. Mani, S., Tardif, N., Rossier, O., Khater, I., Zhou, X., Vicente, F.N., Radhakrishnan, A., Brito, I., Ruez, R., Dewulf, M., et al. (2025). Remote Control of Cell Signaling through Caveolae Mechanics. Nature Cell Biology *Under revision*.

18. Thottacherry, J.J., Kosmalska, A.J., Kumar, A., Vishen, A.S., Elosegui-Artola, A., Pradhan, S., Sharma, S., Singh, P.P., Guadamillas, M.C., Chaudhary, N., et al. (2018). Mechanochemical feedback control of dynamin independent endocytosis modulates membrane tension in adherent cells. Nat Commun *9*, 4217.
19. Tachikawa, M., Morone, N., Senju, Y., Sugiura, T., Hanawa-Suetsugu, K., Mochizuki, A., and Suetsugu, S. (2017). Measurement of caveolin-1 densities in the cell membrane for quantification of caveolar deformation after exposure to hypotonic membrane tension. Sci Rep *7*, 7794.
20. Lolo, F.N., Walani, N., Seemann, E., Zalvidea, D., Pavón, D.M., Cojoc, G., Zamai, M., Viaris de Lesegno, C., Martínez de Benito, F., Sánchez-Álvarez, M., et al. (2023). Caveolin-1 dolines form a distinct and rapid caveolae-independent mechanoadaptation system. Nat Cell Biol *25*, 120-133.
21. Chaudhary, N., Gomez, G.A., Howes, M.T., Lo, H.P., McMahon, K.A., Rae, J.A., Schieber, N.L., Hill, M.M., Gaus, K., Yap, A.S., et al. (2014). Endocytic crosstalk: cavins, caveolins, and caveolae regulate clathrin-independent endocytosis. PLoS Biol *12*, e1001832.
22. Shi, F., and Sottile, J. (2008). Caveolin-1-dependent beta1 integrin endocytosis is a critical regulator of fibronectin turnover. J Cell Sci *121*, 2360-2371.
23. Yeh, Y.-C., Ling, J.-Y., Chen, W.-C., Lin, H.-H., and Tang, M.-J. (2017). Mechanotransduction of matrix stiffness in regulation of focal adhesion size and number: reciprocal regulation of caveolin-1 and β1 integrin. Scientific Reports *7*, 15008.
24. Lolo, F.N., Pavón, D.M., Grande-García, A., Elosegui-Artola, A., Segatori, V.I., Sánchez, S., Trepat, X., Roca-Cusachs, P., and Del Pozo, M.A. (2022). Caveolae couple mechanical stress to integrin recycling and activation. Elife *11*.
25. Monteiro, P., Remy, D., Lemerle, E., Routet, F., Macé, A.-S., Guedj, C., Ladoux, B., Vassilopoulos, S., Lamaze, C., and Chavrier, P. (2023). A mechanosensitive caveolae–invadosome interplay drives matrix remodelling for cancer cell invasion. Nature Cell Biology *25*, 1787-1803.
26. Boscher, C., and Nabi, I.R. (2013). Galectin-3- and phospho-caveolin-1-dependent outside-in integrin signaling mediates the EGF motogenic response in mammary cancer cells. Molecular Biology of the Cell *24*, 2134-2145.
27. Sabharanjak, S., Sharma, P., Parton, R.G., and Mayor, S. (2002). GPI-Anchored Proteins Are Delivered to Recycling Endosomes via a Distinct cdc42-Regulated, Clathrin-Independent Pinocytic Pathway. Developmental Cell *2*, 411-423.
28. Rossatti, P., Ziegler, L., Schregle, R., Betzler, V.M., Ecker, M., and Rossy, J. (2019). Cdc42 Couples T Cell Receptor Endocytosis to GRAF1-Mediated Tubular Invaginations of the Plasma Membrane. Cells *8*.
29. Wong, T.H., Khater, I.M., Joshi, B., Shahsavari, M., Hamarneh, G., and Nabi, I.R. (2021). Single molecule network analysis identifies structural changes to caveolae and scaffolds due to mutation of the caveolin-1 scaffolding domain. Sci Rep *11*, 7810.
30. Hill, M.M., Bastiani, M., Luetterforst, R., Kirkham, M., Kirkham, A., Nixon, S.J., Walser, P., Abankwa, D., Oorschot, V.M., Martin, S., et al. (2008). PTRF-Cavin, a conserved cytoplasmic protein required for caveola formation and function. Cell *132*, 113-124.
31. Hu, M., Zhou, N., Cai, W., and Xu, H. (2022). Lysosomal solute and water transport. Journal of Cell Biology *221*.

32. Roffay, C., Molinard, G., Kim, K., Urbanska, M., Andrade, V., Barbarasa, V., Nowak, P., Mercier, V., García-Calvo, J., Matile, S., et al. (2021). Passive coupling of membrane tension and cell volume during active response of cells to osmosis. Proc Natl Acad Sci U S A *118*.
33. Hamill, O.P., and Martinac, B. (2001). Molecular Basis of Mechanotransduction in Living Cells. Physiological Reviews *81*, 685-740.
34. Du, J., Chen, X., Liang, X., Zhang, G., Xu, J., He, L., Zhan, Q., Feng, X.Q., Chien, S., and Yang, C. (2011). Integrin activation and internalization on soft ECM as a mechanism of induction of stem cell differentiation by ECM elasticity. Proc Natl Acad Sci U S A *108*, 9466-9471.
35. Moreno-Vicente, R., Pavon, D.M., Martin-Padura, I., Catala-Montoro, M., Diez-Sanchez, A., Quilez-Alvarez, A., Lopez, J.A., Sanchez-Alvarez, M., Vazquez, J., Strippoli, R., et al. (2018). Caveolin-1 Modulates Mechanotransduction Responses to Substrate Stiffness through Actin-Dependent Control of YAP. Cell Rep *25*, 1622-1635 e1626.
36. Sigismund, S., Lanzetti, L., Scita, G., and Di Fiore, P.P. (2021). Endocytosis in the context-dependent regulation of individual and collective cell properties. Nature Reviews Molecular Cell Biology *22*, 625-643.
37. Meng, F., Saxena, S., Liu, Y., Joshi, B., Wong, T.H., Shankar, J., Foster, L.J., Bernatchez, P., and Nabi, I.R. (2017). The phospho–caveolin-1 scaffolding domain dampens force fluctuations in focal adhesions and promotes cancer cell migration. Molecular Biology of the Cell *28*, 2190-2201.
38. Kosmalska, A.J., Casares, L., Elosegui-Artola, A., Thottacherry, J.J., Moreno-Vicente, R., González-Tarragó, V., Del Pozo, M., Mayor, S., Arroyo, M., Navajas, D., et al. (2015). Physical principles of membrane remodelling during cell mechanoadaptation. Nat Commun *6*, 7292.
39. Zook, E., Pan, Y.E., Wipplinger, A., Kerschbaum, H.H., Clements, R.J., Ritter, M., Stauber, T., and Model, M.A. (2024). Delayed vacuolation in mammalian cells caused by hypotonicity and ion loss. Scientific Reports *14*, 29354.
40. Li, P., Hu, M., Wang, C., Feng, X., Zhao, Z., Yang, Y., Sahoo, N., Gu, M., Yang, Y., Xiao, S., et al. (2020). LRRC8 family proteins within lysosomes regulate cellular osmoregulation and enhance cell survival to multiple physiological stresses. Proceedings of the National Academy of Sciences *117*, 29155-29165.
41. Reddy, A., Caler, E.V., and Andrews, N.W. (2001). Plasma membrane repair is mediated by Ca(2+)-regulated exocytosis of lysosomes. Cell *106*, 157-169.
42. Corrotte, M., Almeida, P.E., Tam, C., Castro-Gomes, T., Fernandes, M.C., Millis, B.A., Cortez, M., Miller, H., Song, W., Maugel, T.K., et al. (2013). Caveolae internalization repairs wounded cells and muscle fibers. Elife *2*, e00926.
43. Corrotte, M., Cerasoli, M., Maeda, F.Y., and Andrews, N.W. (2020). Endophilin-A2-dependent tubular endocytosis promotes plasma membrane repair and parasite invasion. J Cell Sci *134*.
44. Pu, W., Qiu, J., Nassar, Z.D., Shaw, P.N., McMahon, K.A., Ferguson, C., Parton, R.G., Riggins, G.J., Harris, J.M., and Parat, M.O. (2020). A role for caveola-forming proteins caveolin-1 and CAVIN1 in the pro-invasive response of glioblastoma to osmotic and hydrostatic pressure. J Cell Mol Med *24*, 3724-3738.

45. Wong, T.H., Khater, I.M., Joshi, B., Shahsavari, M., Hamarneh, G., and Nabi, I.R. (2020). Super-resolution network analysis detects structural alteration of caveolae and scaffolds due to point mutation of the Cav1 scaffolding domain. In preparation.
46. Timmins, L.R., Ortiz-Silva, M., Joshi, B., Li, Y.L., Dickson, F.H., Wong, T.H., Vandevoorde, K.R., and Nabi, I.R. (2024). Caveolin-1 promotes mitochondrial health and limits mitochondrial ROS through ROCK/AMPK regulation of basal mitophagic flux. The FASEB Journal *38*, e23343.
47. Gao, G., Zhu, C., Liu, E., and Nabi, I.R. (2019). Reticulon and CLIMP-63 regulate nanodomain organization of peripheral ER tubules. PLoS Biol *17*, e3000355.
48. BOLTE, S., and CORDELIÈRES, F.P. (2006). A guided tour into subcellular colocalization analysis in light microscopy. Journal of Microscopy *224*, 213-232.

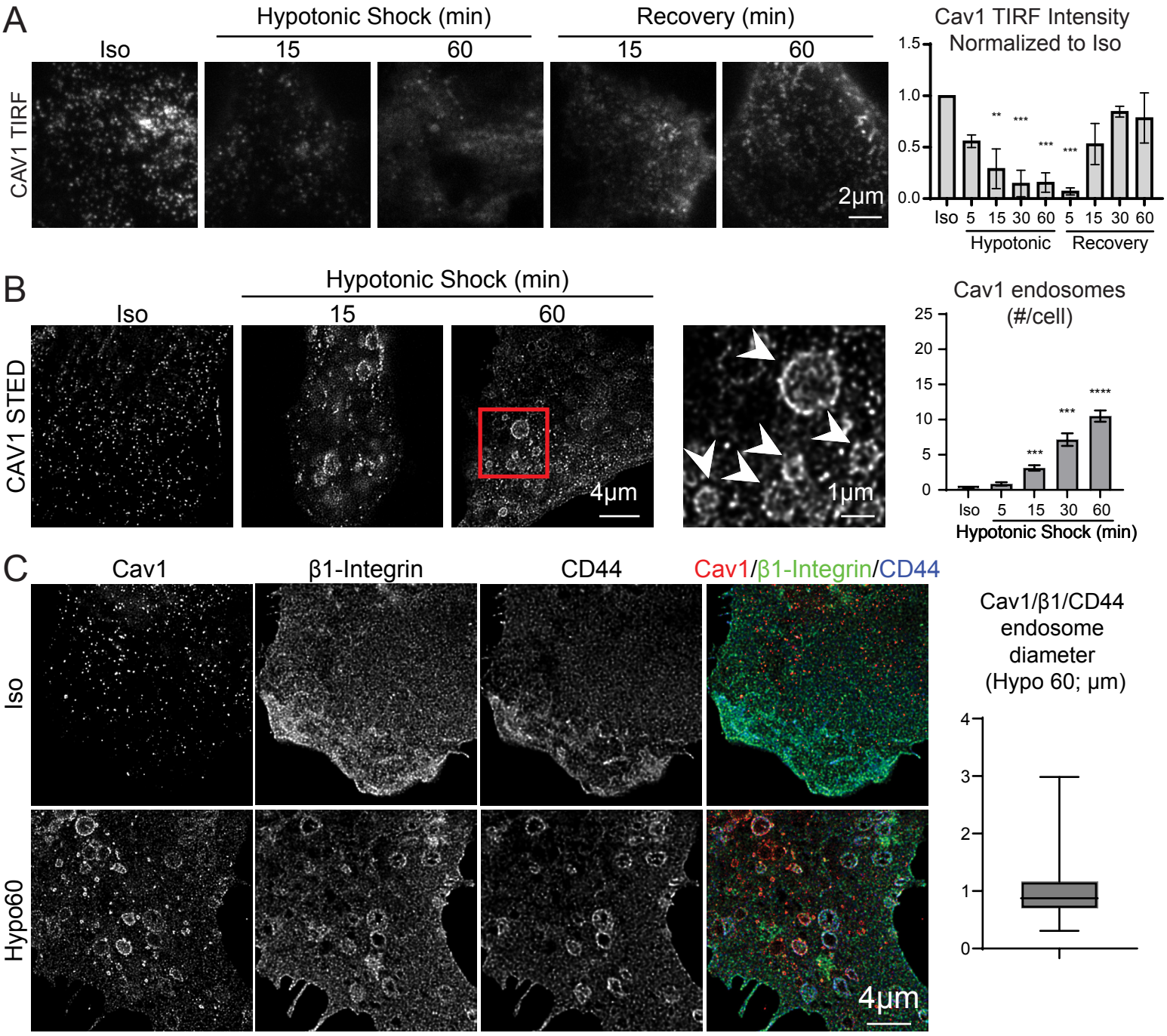

Wong et al Figure 1

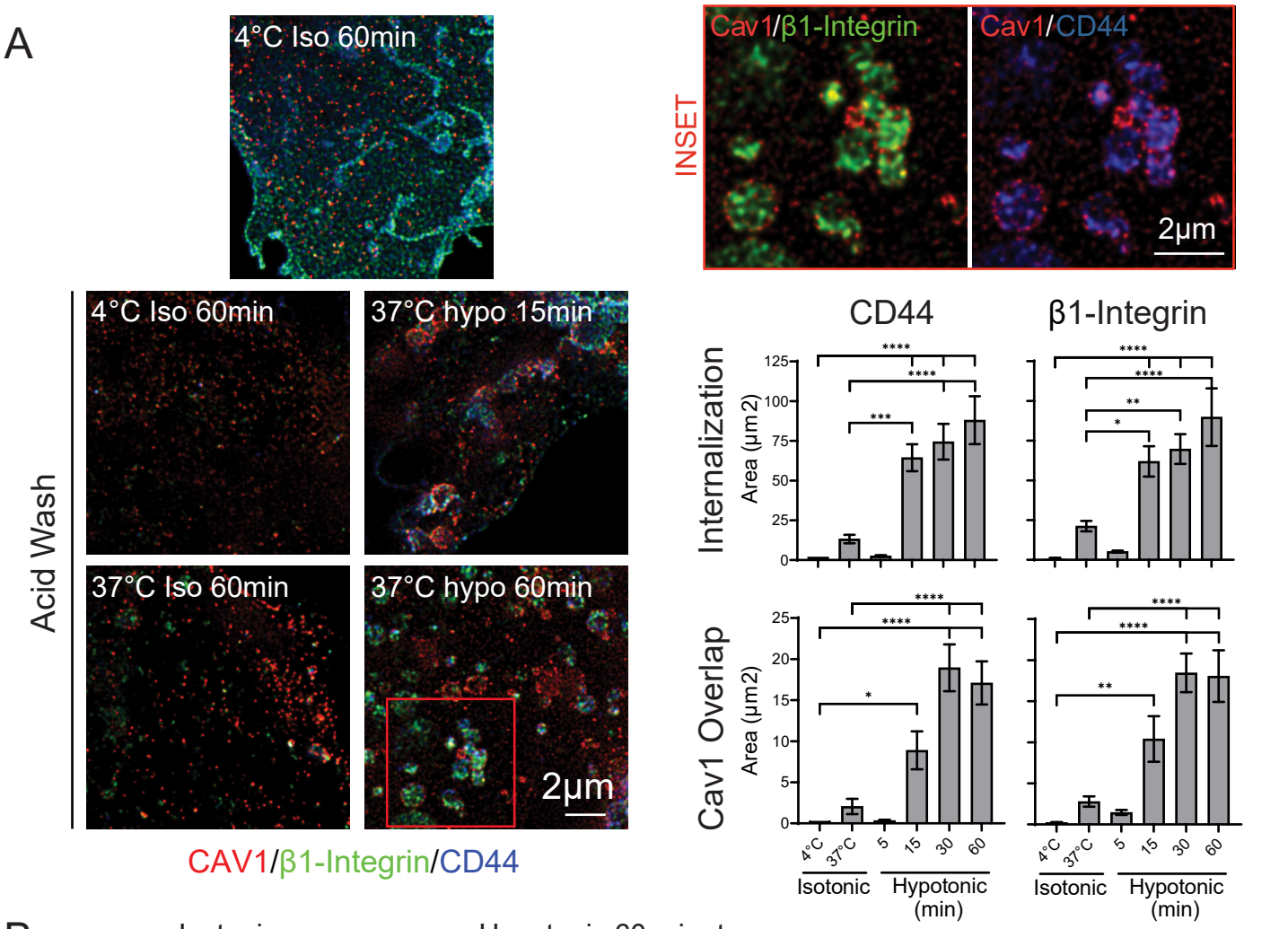

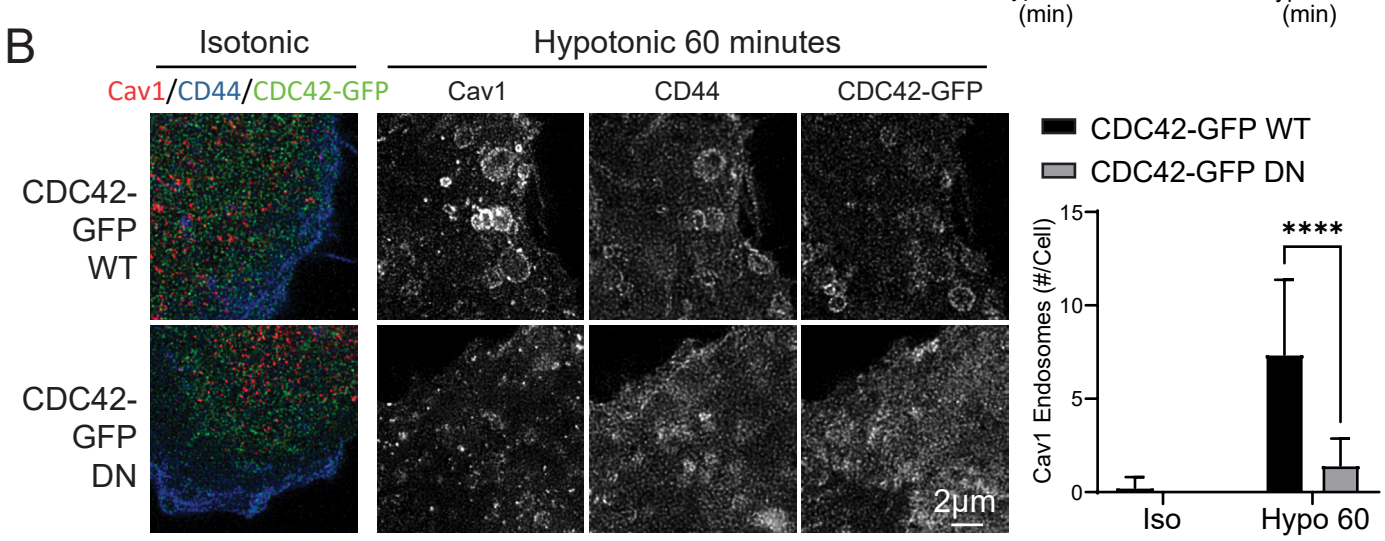

Wong et al Figure 2

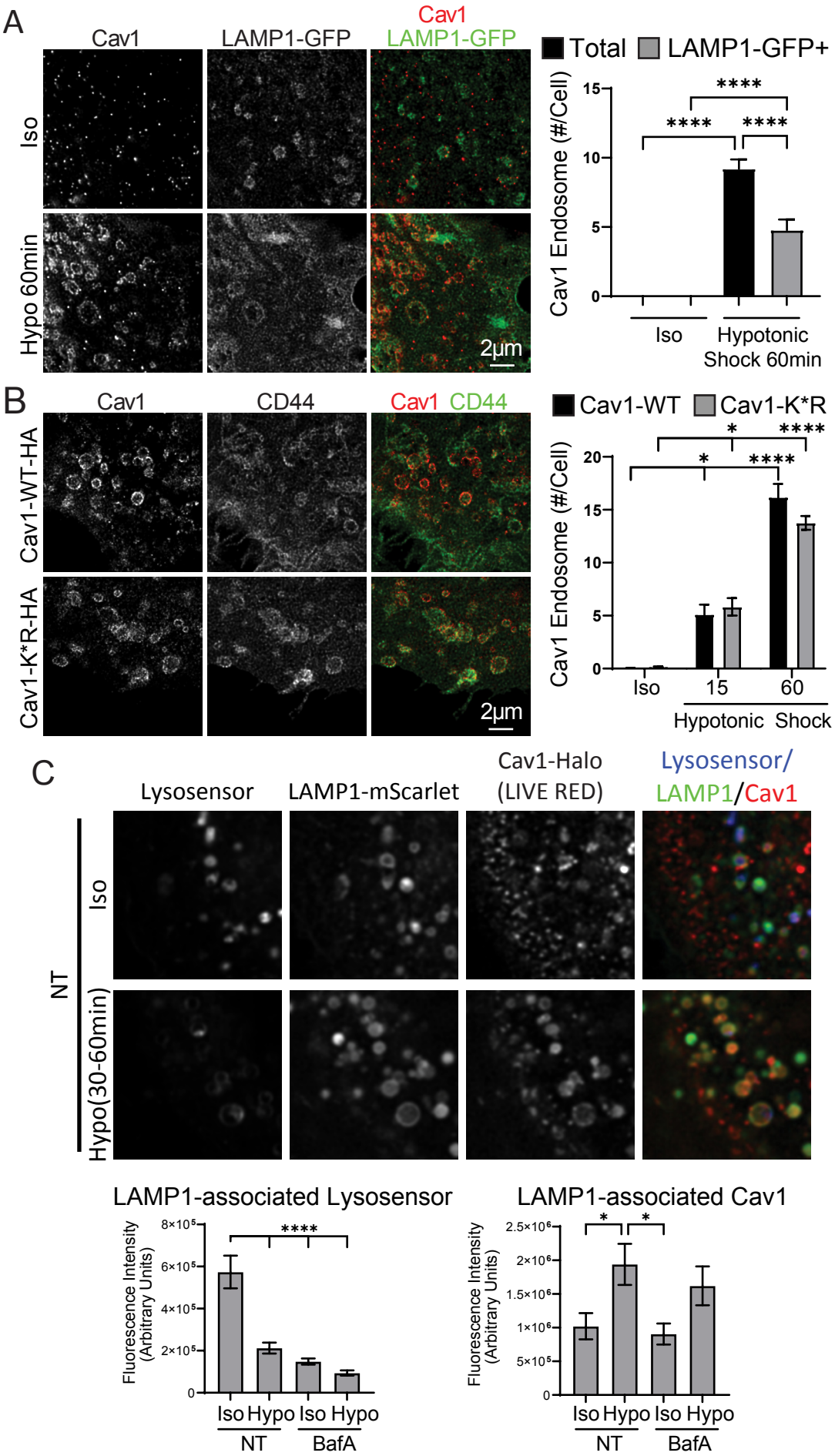

Wong et al Figure 3

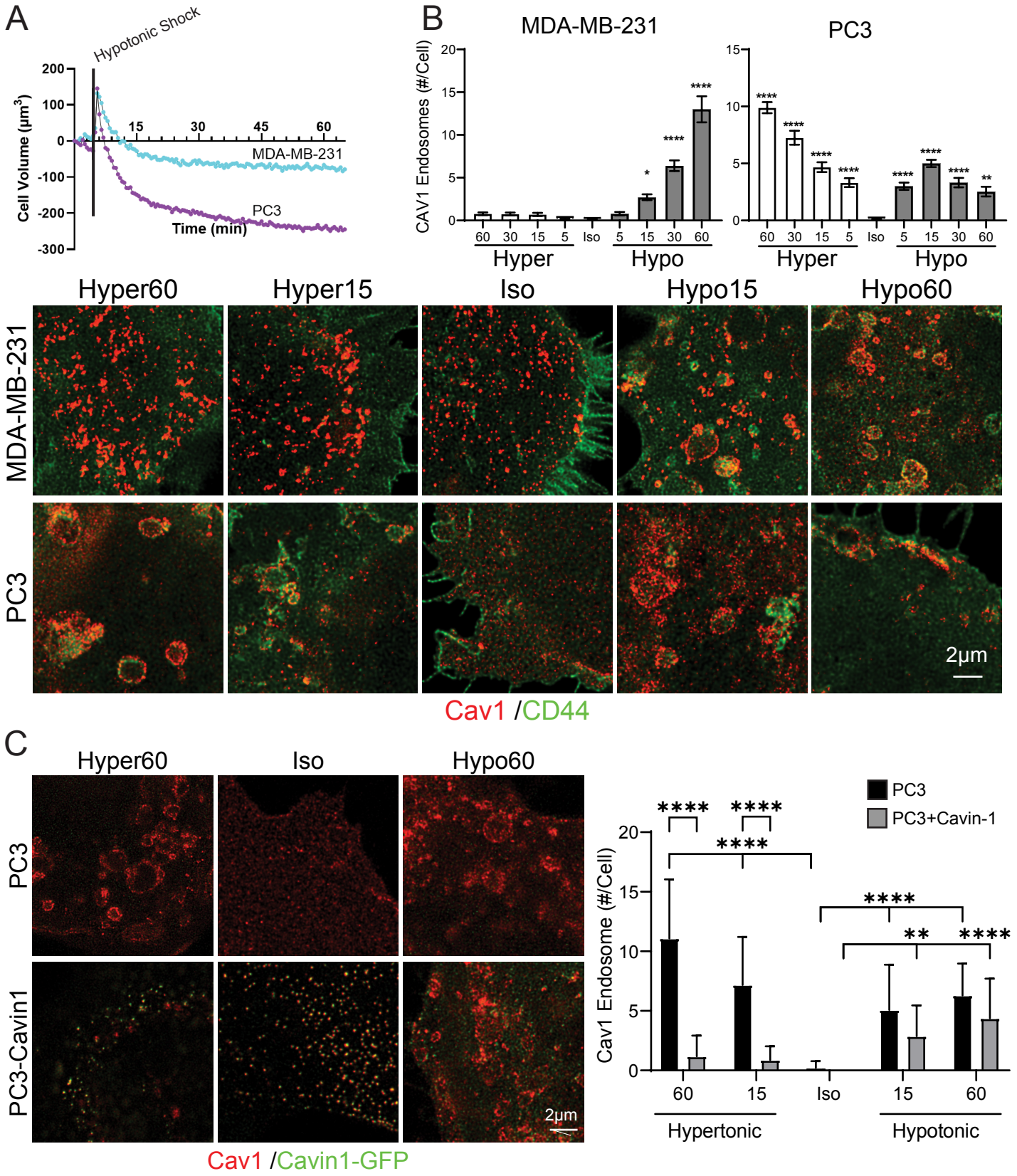

Wong et al Figure 4